Proceedings World Geothermal Congress 2010
Bali, Indonesia, 25-29 April 2010

Analysis of Spatial and Temporal Evolution of the Ground Deformation in the Cerro Prieto Geothermal Field (Mexicali Valley, B.C., Mexico) Using DInSAR and Leveling Data

Olga Sarychikhina, Robert Mellors and Ewa Glowacka

C I C E S E, Km. 107 Carretera Tijuana – Ensenada, 22860, Esenada, B.C., México

osarytch@cicese.mx, rmellors@geology.sdsu.edu, glowacka@cicese.mx

Keywords: Cerro Prieto, geothermal fields, ground deformation, DInSAR, leveling.

ABSTRACT

Geodetic monitoring of the Cerro Prieto Geothermal Field (Mexicali Valley, B.C., Mexico) and the surrounding area has been historically carried out with ground-based surveys. These surveys provide information only at a number of measuring points. The surveys are time-consuming and expensive and restricted by available resources. These limitations could be relieved by exploiting the satellite-based differential interferometry (DInSAR) which allows the extraction of geodetic information over wide area and yielding improved coverage in comparison with the mean repetition time of the campaign measurements.

Recent results from Cerro Prieto Geothermal Field (CPGF), obtained from ENVISAT ASAR descending data from October 2003 – March 2006 are shown in this work. The results reveal that the area of the CPGF is continuously subsiding. A stack of 4 interferograms spanning the 350 day time-period between December 2004 and December 2005 indicates a maximum subsidence velocity of at least 15 cm/yr. Comparison of subsidence maps obtained from DInSAR data for the indicated period and from leveling data for the 1994-1997 period allows the evaluation of changes both in the spatial pattern and in the rate of subsidence. These changes are compared to the production development in the CPGF.

1. INTRODUCTION

Ground subsidence is an expected consequence of the production of geothermal fluids and steam. Fluid removal from subsurface reservoirs in the form of geothermal water and brine produces a compaction of the depleted formations which migrates totally or partially to the ground surface, thus inducing anthropogenic land subsidence. Surface deformation is observed even in kilometers deep reservoirs isolated from shallow groundwater. Surface subsidence rates of up to dozens of centimeters per year have been measured across several major geothermal fields (e.g., Wairakei, New Zealand (Allis *et al.*, 1998), Geysers, USA (Mossop and Segal, 1997)).

Traditional measurements of land subsidence have been carried out using geodetic methods such as precise leveling and geotechnical instruments such as tiltmeters. Recently, GPS (Global Positioning System) surveys have been used. All of these techniques (1) measure changes in locations with a limited set of benchmarks, (2) require a large number of individual observations to map the subsidence distribution, (3) require ground access, and (4) are generally costly to acquire. The Differential Interferometric Synthetic Aperture Radar (DInSAR) technique has been widely adopted to monitor land subsidence caused by withdrawal of water, oil, gas, and other minerals. The main advantage of DInSAR is its ability to provide high resolution (up to a few tens of meters) maps of crustal deformation with large spatial coverage (~100×100 km) at subcentimeter accuracy (Bürgmann *et al.*, 2000; Hansen 2001).

The results of ground deformation studies for the Cerro Prieto Geothermal Field and surrounding areas in the Mexicali Valley, which employed the methods of conventional two-pass DInSAR and stacking of conventional interferograms, are presented in this work. The period covered by the analyzed images is October 2003 – March 2006. A serie of differential interferograms spanning the 350 day time-period between December 2004 and December 2005 was obtained. Finally, in an attempt to evaluate the changes in the spatial pattern and rate of land subsidence, comparison to available leveling data from the 1994-1997 period was performed.

2. STUDIED AREA

The Cerro Prieto Geothermal Field, which is situated in Mexicali Valley, Baja California, Mexico, has been exploited for energy production since the 1973. Since then, production growth has been achieved by increasing the number of power plants and wells. At present, CPGF is the world's second largest geothermal field. The latest increase in production is due to the development of a new power plant (CP IV) to the northeast of existing plants since 2000.

The subsidence history at the CPGF area has been well documented. Geodetic studies in the Mexicali Valley began in the 1960's. Ground deformation in the studied area has been monitored using repeat ground surveys with precise leveling and GPS (mainly conducted by the Mexican Federal Electricity Commission) and is currently monitored with quasi continuous records of the geotechnical instruments network (tiltmeters and extensometers) maintained by CICESE and CONACYT. The analysis of measurements from the leveling surveys done in the area of CPGF and the Mexicali Valley from 1977 to 1997 and geotechnical instruments installed in the area in 1996 showed that the extension and shape of the subsidence zone were originally controlled by tectonics; however, the current subsidence rate is mainly related to fluid extraction (Glowacka *et al.*, 1999; Glowacka *et al.*, 2005, Suarez-Vidal *et al.*, 2008).

Subsidence in the CPGF was also measured via DInSAR by Carnec and Fabriol (1999) and Hanssen (2001) using ERS1/2 images acquired from 1993 – 1997 and 1995-1997, respectively. This subsidence was interpreted as being caused by geothermal fluid extraction.

3. DINSAR DATA ANALYSIS

This study started with the analysis using conventional two-pass DInSAR. Seventeen ENVISAT SAR images of the study area were acquired from October 2003 to March 2006

in descending pass (track 84, frame 2961) by the European Space Agency (ESA). The spatial coverage of these images is presented in Figure 1. The details of the interferometric pairs presented in this paper are given in the Table 1.

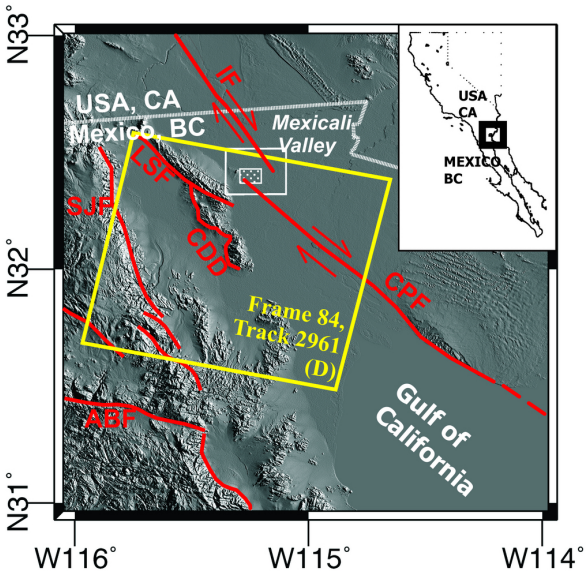

Figure 1: Regional map of the study area. SRTM DEM is used as the background. The large yellow rectangle indicates the spatial coverage of ENVISAT track along which SAR data were recollected. D indicates descending track. The white rectangle represents the study area. The area of CPGF (Cerro Prieto Geothermal Field) is represented by the smaller filled rectangle. The principal tectonic faults are also indicated: Cerro Prieto Fault (CPF), Imperial Fault (IF), Agua Blanca Fault (ABF), Sierra Juarez Fault (SJF), Laguna Salada Fault (LSF) and Cañada David Detachment (CDD).

Table 2: Interferometric pairs. All SAR images are from ENVISAT satellite, descending pass, track 84, frame 2961.

Pairs	Image 1	Image 2	B_{temp} (days)	$B_{\perp}$ (m)
a	2004/12/19	2005/02/27	70	112
b	2005/02/27	2005/06/12	105	-53
c	2005/06/12	2005/09/25	105	206
d	2005/09/25	2005/12/04	70	-260
e	2005/05/08	2005/10/30	175	-160
f	2003/10/26	2004/10/10	350	-147

Interferometric processing was performed using the public domain DORIS InSAR package developed at the Delft Institute for Earth-oriented Space Research (Kampes *et al.*, 2003). The interferograms were corrected for the phase signature due to orbital separation using precise DEOS satellite orbits (Scharroo and Visser 1998) and for the topography using a 3-arcsecond Shuttle Radar Topography Mission (SRTM) digital elevation model. The signal-to-noise ratio of each differential interferogram was improved using the Goldstein adaptive phase filter (Goldstein and Werner, 1998). All DORIS InSAR products were formed applying a complex multi-look operation with 4 and 20 looks in range and azimuth, respectively, resulting in a final pixel size of approximately 100m by 100m.

Firstly, sixty-five interferometric pairs with perpendicular baselines less than 400 m were selected from the total 136 pairs formed from the combinations of the 17 acquisitions. The most incoherent interferograms were rejected by limiting the baseline. Subsequently, these 65 pairs were visually analyzed to identify the pairs affected by strong phase noise and atmospheric effects. It was found that, in spite of having a short perpendicular baseline, several differential interferograms present a high level of phase noise due to temporal decorrelation of the signal, induced by variations in the dielectric properties of the targets, between the two acquisitions.

The highly vegetated CPGF surrounding areas cause significant phase decorrelation of SAR couples over periods longer than 3 months due to the seasonal growth and movements caused by the wind on the grown plants, while the mainly desert CPGF area maintains high levels of coherence over longer time intervals. These interferograms are shown in Figure 2.

In addition to the spatial and temporal decorrelation, the accuracy of deformation rate estimation from individual differential interferograms was limited by the atmospheric path delay term. The main element confirming that the observed signature was not related to atmosphere is the persistence of the signature on different independent interferograms. The assumption is that the deformation phase is highly correlated and the error terms (atmosphere, signal noise, and related baseline) are uncorrelated between the independent pairs.

Six geocoded differential interferograms are shown in Figure 2, which were constructed using the two-pass method in this study. Each fringe cycle in the differential interferogram corresponds to half the radar wavelength of the apparent range change (28 mm in the case of ENVISAT satellite data) in satellite-to-ground line of sight (LOS) direction. All differential interferograms show essentially the same fringe pattern. Therefore, the observed fringes are not due to atmospheric effects, but represent ground deformation that must have occurred during the periods spanned by the presented differential interferograms. The elliptical northeast-southwest directed fringe pattern indicates an increase in range. The relatively steep look angle of the ENVISAR radars (~23°) and the evidence for vertical displacement in the study area from ground-truth observations (including leveling measurements) suggest that the observed range increase is mostly due to surface subsidence.

In all short-term differential interferograms (Figure 2 a-d), the elliptical area with the highest deformation rate has two subsidence basins: the first center of subsidence is located below the CPGF production zone, and the second is located in the area between the eastern limits of the CPGF and the Saltillo Fault, which was proposed as a recharge zone in previous studies (Glowacka *et al.*, 1999; Sarychikhina, 2003). Despite the high phase decorrelation level of the interferometric pairs covering longer time intervals (Figure 2 e-f), the same fringe pattern can be visually traced. The contours of the fringes show an elliptic subsidence basin bellow the CPGF production zone.

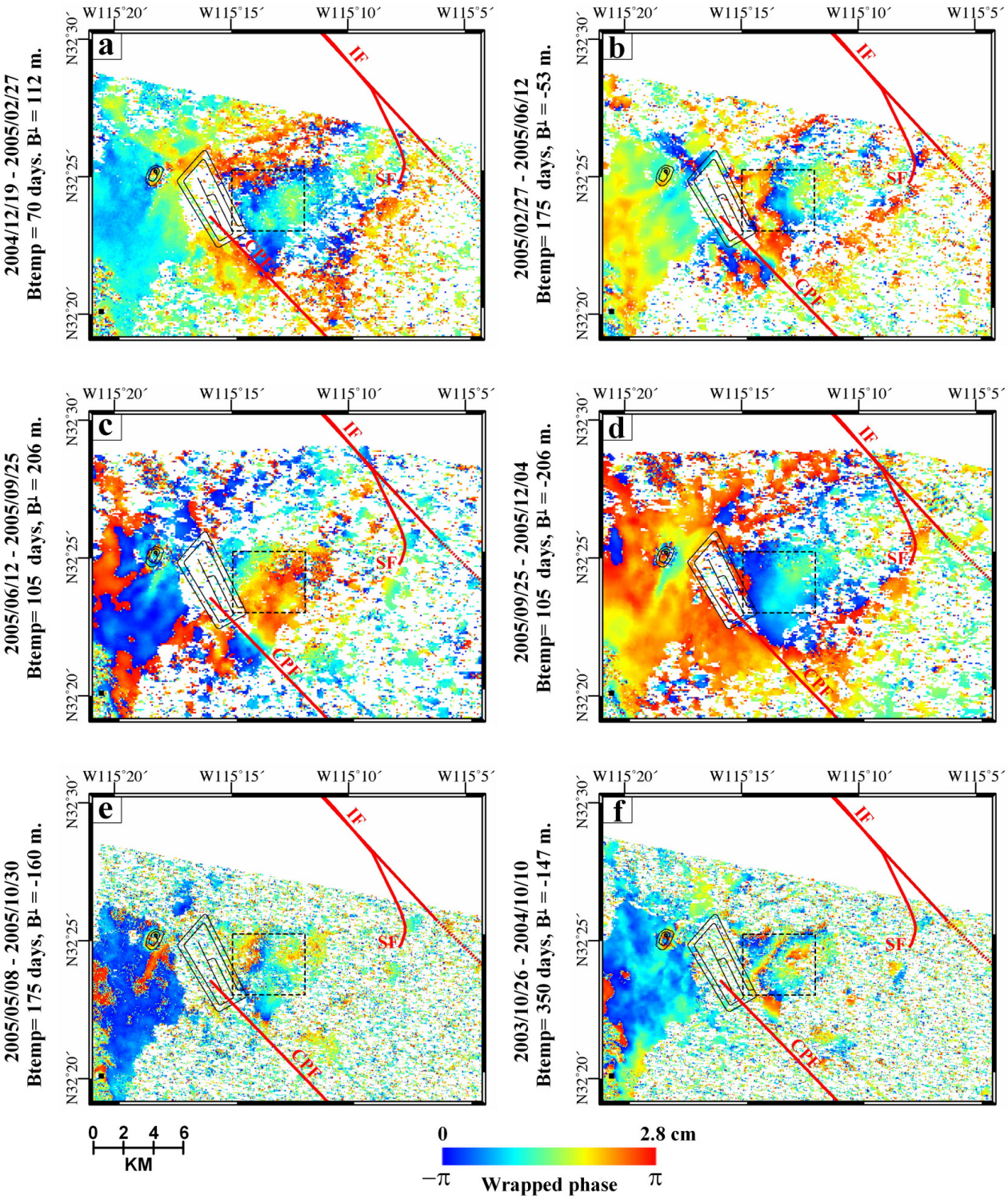

Figure 2: Six differential (wrapped) interferograms for the study area, showing spatial and temporal distribution of ground deformation in the study area. Areas of low coherence (<0.1) are masked.CPF denotes Cerro Prieto Fault, IF the Imperial Fault, SF the Saltillo Fault. The black dotted rectangle marks the CPGF extraction zone. The borders of the evaporation pond and the Cerro Prieto volcano are superimposed on the images for orientation.

In order to calculate the yearly rate of deformation, a simple differential interferogram stacking method was applied. Stacking differential interferograms involves summing of multiple differential interferograms into a single interferogram. This is useful for overcoming the two shortcomings of conventional DInSAR, which are the low coherence over long temporal separations and the atmospheric influence. The four best differential interferograms of successive periods with temporal separations between 70 and 105 days were selected, and are shown in Figure 2 a-d.

The phase of each interferogram was first unwrapped using a statistical minimum-cost flow algorithm implemented in

the SNAPHU package (Chen and Zebker, 2001), converted to the LOS displacement, and referenced to a common point in space, which is the fixed point for the leveling 1994-1997 data. The resulting from the stacking LOS displacement map covered the 350 days long period between December 2004 and December 2005. The map of the deformation rate, in cm/year, which can be viewed as a displacement velocity map, is shown in Figure 3a. As it can be seen in the Figure 3a, the maximum rate of the deformation was estimated to be ~16 cm/yr and is observed in the recharge zone. The maximum deformation rate in the CPGF production zone is ~10 cm/yr. Relatively strong deformation rate gradients were observed to the south of an evaporation lagoon near the northern end of the Cerro Prieto Fault and in the eastern part of the study area near the Saltillo Fault that suggest than the ground deformation area is bounded in west and east, respectively, by those geological structures.

4. DISCUSSION

The leveling 1994-1997 results (Glowacka *et al.*, 1999, Glowacka *et al.*, 2005) and the DInSAR data from the stacked interferograms were compared to evaluate the changes in the spatial pattern and rate of land subsidence. The leveling data projected to the LOS direction are shown in the Figure 3b. The leveling data showed a maximum deformation rate of 12 cm/yr below the center of the CPGF production zone and 9 cm/yr below the recharge zone. This comparison of deformation rates obtained from different techniques and time intervals indicates that the average rate of deformation has increased since 1997. The maximum increase in the deformation rate is observed below the recharge zone. The center of deformation below the CPGF production zone is migrating to the northeast. The changes in the ground deformation pattern may be caused by production development in the CPGF due to the newest power plant (CP IV), which started operating in 2000 in the eastern part of field (Sarychikhina *et al.*, 2007 and Glowacka *et al.*, 2009).

5. CONCLUSIONS

Differential interferometric analysis of space-borne ENVISAT SAR was used to map land subsidence in the CPGF and surrounding areas in the Mexicali Valley in northwestern Mexico. DInSAR observations reveal that the total area of subsidence appears as a roughly NE-SW oriented elliptical-shaped feature with two bowls exhibiting high deformation rates in the December 2004–December 2005 period: ~16 cm/yr below the recharge zone (east – northeast of the study area) and ~10 cm/yr below the east boundary of CPGF production zone. The analysis of DInSAR data shows that, despite several limitations associated with the application of this method, the radar data provided a detailed mapping of both the amplitude and spatial extent of land subsidence in the study area. In particular, the DInSAR mapping reveals that the tectonic faults control the spatial extent of the observed subsidence along its western and eastern margin.

Comparison of the radar observations of land subsidence to leveling observations from the 1994-1997 period revealed changes in both spatial pattern and subsidence rate. These changes could be related to the production development in the CPGF and suggest that the land subsidence in the study area is a dynamical process.

6. ACKNOWLEDGEMENT

The European Space Agency's ENVISAT satellite was used to collect the interferometric data. The data were obtained as part of ESA Cat-1 Project (ID - C1P3508).

This research was sponsored in part by CONACYT, project number 45997-F, and CICESE internal funds. The first author was sponsored by the Ministry of Foreign Affairs of Mexico (SRE) PhD scholarship.

The opinions expressed in this paper are solely the authors' and do not necessarily express the point of view of Mexican Federal Electricity Commission which operates CPGF.

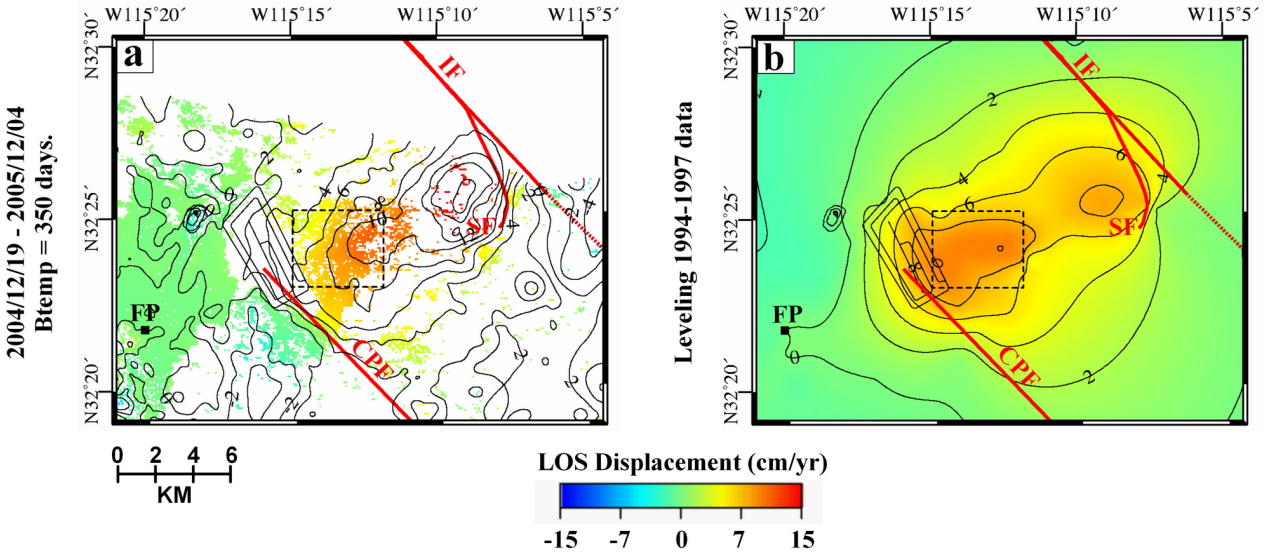

Figure 3: a) LOS displacement rate (cm/yr) obtained by stacking 4 differential interferograms from the December 2004 - December 2005 period. Areas of low coherence (<0.1) are masked. b) LOS displacement rate (cm/yr) obtained from a leveling survey during the 1994-1997 period. CPF denotes the Cerro Prieto Fault, IF the Imperial Fault, SF the Saltillo Fault. The black dotted rectangle marks the CPGF extraction zone. The borders of the evaporation pond and the Cerro Prieto volcano are superimposed on the images for orientation. FP is the fixed reference point.

REFERENCES

Allis, R. G., Zhan X. and Clotworthy A.: Predicting Future Subsidence at Wairakei Field, New Zealand, *Geothermal Resources Council Trans.*, **22**, (1998), 43-47.

Bürgmann, R., Rosen, P.A. and Fielding, E.J.: Synthetic aperture radar interferometry to measure earth's surface topography and its deformation, *Ann. Rev. Earth planet. Sci.*, **28**, (2000), 169–209.

Carnec, C. and Fabriol, H.: Monitoring and modeling land subsidence at the Cerro Prieto geothermal field, Baja California, Mexico, using SAR interferometry, *Geophysical Research Letters*, **26 (9)**, (1999), 1211-1214.

Chen, C. W., and Zebker H. A.: Two-dimensional phase unwrapping with use of statistical models for cost functions in nonlinear optimization, *Journal of the Optical Society of America*, **18**, (2001), 338-351.

Glowacka E., J. Gonzalez, Fabriol H.: Recent Vertical deformation in Mexicali Valley and its Relationship with Tectonics, Seismcity and Fluid Operation in the Cerro Prieto Geothermal Field, *Pure and Applied Geophysics*, **156**, (1999), 591-614.

Glowacka E., Sarychikhina O., Nava A.F.: Subsidence and stress change in the Cerro Prieto Geothermal Field, B.C., Mexico, *Pure and Applied Geophysics*, **162**, (2005), 2095-2110.

Glowacka E., Sarychikhina O., Suarez-Vidal F., Nava Pichardo F.A., Mellors R.: Anthropogenic subsidence in the Mexicali Valley, Baja California, Mexico, and slip on the Saltillo fault, *Environmental Earth Sciences*, (2009), doi:10.1007/s12665-009-0137-y.

Goldstein, R.M. and Werner C.L.: Radar interferogram filtering for geophysical applications, *Geophysical Research Letters***, 25 (21)**, (1998), 4035-4038.

González, J. J., Glowacka, E., Suárez, F., Quiñónez, G., Guzmán, M., Castro, J. M., Riviera, F., and Félix, M. G.: Movimiento reciente de la falla Imperial, Mexicali, B. C., *Divulgare, Ciencia para todos, Mexicali, B. C.* **6 (22)**, (1998), 4-15.

Hanssen, R. F.: Radar Interferometry: Data Interpretation and Error Analysis, Kluwer Academic Publishers, Dordrecht, Netherlands (2001).

Kampes, B., Hanssen R., and Perski Z.: Radar interferometry with public domain tools, in *Proceedings of FRINGE 2003*, 1–5 December, Frascati, Italy (2003).

Mossop, A. P. and Segall P.: Subsidence at the Geysers geothermal field, N. California from a comparison of GPS and leveling surveys, *Geophysical Research Letters*, **24**, (1997), 1839 – 1842.

Sarychikhina, O.: Modelación de subsidencia en el campo geotérmico Cerro Prieto, *M.S. thesis*, CICESE, B.C., México (2003).

Sarychikhina, O., Glowacka E. and, Mellors R.: Preliminary results of a surface deformation study, using differential InSAR technique at the Cerro Prieto Geothermal Field, B.C., Mexico, *Geothermal Resources Council Trans*,. **31**, (2007), 581-584.

Scharoo, R., and Visser P.: Precise orbit determination and gravity field improvement for the ERS satellites, *Journal of Geophysical Research* **103 (C4)**, (1998), 8113-8127.

Suarez-Vidal F, Mendoza-Borunda R., Naffarrete-Zamarripa L.M., Ramirez J., Glowacka E.: Shape and dimensions of the Cerro Prieto pull-apart basin, Mexicali, Baja California, México, based on the regional seismic record and surface structures, *International Geology Review*, **50 (7)**, (2008), 636-649.